International Journal of Engineering & Technology, 7 (4.27) (2018) 16-21

International Journal of Engineering & Technology

Website: www.sciencepubco.com/index.php/IJET

Research paper



Impedance Control Approach on Leg Motion Speed Variation on Soft Surface Interaction

Wan Mohd Nafis Wan Lezaini[1]*, Addie Irawan [2] and Akhtar Razul Razali [3]

[1]Robotics and Unmanned Systems (RUS) group, Faculty of Electrical & Electronics Engineering, Universiti Malaysia Pahang, Pahang, Malaysia
[2]Manufacturing Focus Group (MFG), Faculty of Mechanical Engineering, Universiti Malaysia Pahang, Pahang, Malaysia
**Corresponding author E-mail: wannafis93@gmail.com*

Abstract

This article presents the leg speed variation control using impedance control approach on soft surface displacement motion. One of the challenging fields of designing a legged robot that can be equipped with adaptation ability is it dynamic control which majorly involved in interaction with the environment. Numerous researchers have been widely implemented impedance control as dynamic interaction but less emphasized in adapting soft terrain. Most of the impedance control implementation on the legged robot on rough terrain emphasized on position changes, and it may not practical for legged robot navigate on the soft terrain. Soft terrain contains different ground stiffness and medium viscosities. Thus, this study has taken the initiative to propose a speed variation control on a robot's leg by using a force-based impedance control approach to increase the leg energy exchanges specifically on foot placement. The proposed control was validated in actual robot's leg, and performances show that the energy in the leg increases as the velocity of leg motion increase due to increase in force feedback while maintaining the shape of the leg motion.

Keywords: *Energy; Impedance Control; Legged Robot; Mobile Robot; Speed Variation of Motion.*

1. Introduction

Numerous ideas have been introduced and presented to confront challenges in designing bio-inspired legged robot according to its needs in the field of applications such as COMET-IV [1], TITAN-XIII [2], CR200 [3] and HyQ [4]. These are several examples of successful design robot that comes with different actuation system, legged mechanism, gait pattern as well as adaption to the environment. Furthermore, these bio-inspired robots are progressively extending their capabilities in the field of application with many settings including robot-environment interaction (dynamic). Similar to cases in the manipulator, the legged robot also needs interaction between its legs and the surrounding environment for both foot placement and perception, specifically in complex terrain that may have unpredictable obstacles or having variable ground stiffness. Controlling the impacts during leg landing on the surface are the key to maintain robot body stability.

Thus, to achieve stability and adaptability of the legged robot during locomotion, an addition of compliance into motion control is vital which will allow the legged robot to have compliance characteristic with the environment. Two options are provided for the robots to have compliance with the environment, which are passive and active compliance. Reconstructing the robot structure especially on the leg design, changing the actuation system of the leg's joint or adding compliant devices such as springs and dampers are methods involved in obtaining passive compliance. Contrary to passive compliance, constructing force feedback of end effector or torque feedback on joints of the robot's leg to control the system behavior actively are the ways to achieve compliance. For instances, explicit force control and impedance control [5]. In explicit or direct force control method, the controller directly controls the force exerted on the surrounding environment using force error tracking to achieve desired force feedback. As presented in [6, 7] where both used Proportional, Integral, and Derivative (PID) closed-loop control in force error tracking in manipulation systems, thus the system yielded same force as the desired force. It is different to the impedance control in which the method emphasizes controlling the force indirectly by regulating the desired relationship between end-effector force or joint torque of the leg to the behavior of robot motion where it is adjusting the mechanical impedance of the end-effector/joint based on the external forces [8].

Moreover, this controller is a framework that commonly used to offer compliant walking for the legged robot since it is a combination of control algorithms that capable to deal with both situations of constraint and free spaces. As the system in free space, it allows the position control to perform precise trajectory tracking since there is no interaction with the environment. As the system in constraint space, the impedance control took place and behave compliantly to the environment as the interaction occurs.

There are two approaches in designing and implementation of impedance control; the force-based impedance or position-based control. Two loops involved in position-based impedance control structure which are inner position loop and outer force loop. During system at free space, this scheme act as open-loop by executing position control and as the system is in constraint space, the scheme becoming close loop control allowing force control to be executed to improve interaction between it end-effector and environment. As reported [9] and [10], each represented hexapod walking robots and hydraulic quadruped robot respectively are the examples of a successful legged robot that implemented position-

Copyright © 2018 Wan Mohd Nafis Wan Lezaini et al. This is an open access article distributed under the Creative Commons Attribution License, which permits unrestricted use, distribution, and reproduction in any medium, provided the original work is properly cited.

based impedance control as active compliance control strategy to the robot's legs. On the contrary, the force-based impedance control scheme equipped with an inner-force loop. For example, LittleDog from Boston Dynamics implemented torque-based impedance control, which also in the same category as force-based impedance control [11]. Whereas, as reported in [12], a hydraulic quadruped namely as HyQ was established based on leg's joint torque-based impedance control without using any mechanical compliant, has successfully demonstrated an excellent squat jump and resonant hopping. MIT Cheetah robot [13] also used the same approached and able to establish a stable running gait. On the other hand, COMET IV [14] a hydraulic hexapod used force-based impedance control to select best step for each of its legs during locomotion on uneven terrain. Similar to the Weaver, electric drive hexapod from CSIRO [15] used the same method to actively leveling its leg while on uneven terrain as well as on the inclination surface.

As abovementioned, many successful legged robots that implemented impedance control only focusing to dynamically changed the trajectory during contact with the environment and has been successfully demonstrated on unstructured terrain while remaining stable during the walking phase. Moreover, several researchers are also applying methods above specifically in hydraulic type robot to achieve desired joint torque or force exerted to the environment using force correction. Two critical sequences in the robot's leg locomotion trajectory are required; lifting and drag sequences. A legged robot that navigates on soft terrain such as mudflat may face different ground stiffnesses, and this will require imparting more force onto environment to overcome the ground stiffness. Otherwise, the leg may sink into the medium as shown as an example scenario in Figure 1.

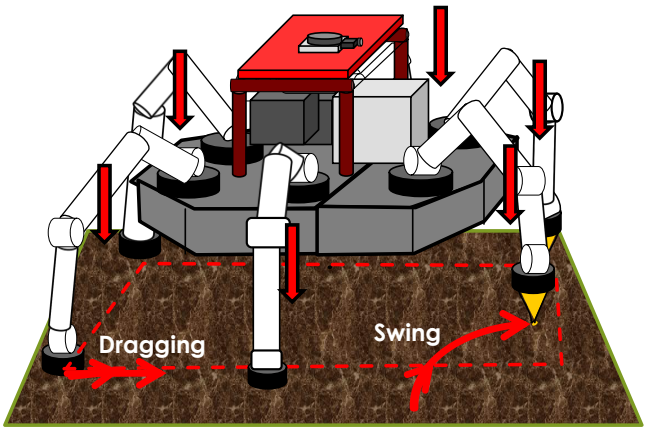

Fig. 1: Legged robot walk on the mudflat

Different to lift to swing sequence that requires robot's leg only to swing leg toward or outward the robot's body for the new location of leg placement, the drag sequence play an important role in moving the robot's body from one place to another via imparting force to the environment. As the ground stiffness increases, it will result in difficulties for the robot to move since the leg was unable to overcome the obstacle. For the robot that fails to move, it might fall to the ground since during this time; the position control is still completing trajectory tracking and skipping several steps in sequence due to the mechanical not responding while getting stuck in the medium. Hence, this paper proposed leg dragging motion speed control, especially for the electric-driven legged robot by using force-based impedance control with aim to increase the speed of the motion based on the force on contact, so that position control produces a larger control output, *u(t)* to the electric driven actuator due to more massive position error. The main objective of this method is to increase the energy of the leg so that it can overcome the above situation, especially during drag sequence. Section 2 showed an overview of the platform used in this study. Section 3 explained the control scheme and proposed a method for this platform whereas section 4 presented and discussed the results obtained for this proposed method.

2. Overview of Mechanism and Kinematics of Hexaquad Robot's Leg

Hexaquad, a biomimetic multi-legged robot named after it capabilities to change configuration between hexapod and quadruped [16], aim to conduct maximum 90 kg payload pick-and-place tasks and to be operated on the riverbed or seabed. Hexaquad was inspired by arthropod configuration (hexapod and quadruped capabilities) and peristaltic creatures (body extending/retracting), where its center set of the leg can move in any direction toward either two ends pair of the leg during in quadruped mode as portrayed in Figure 2. For each of Hexaquad's leg, the actuators specifications for each joint are listed in Table 1. The bipolar stepper motor is set to drive joint 1 while two linear actuator motors drive joint 2 and 3 of Hexaquad's leg. Moreover, the abilities to transform from foot-to-gripper (FTG) were installed on each of the leg's tip and controlled by a tubular actuator motor. The Hexaquad's leg was designed with underactuated configuration. However, since the actuator of each link was influenced by a joint sensor connected directly to each joint, hence, its orientation is assumed to be direct actuation with the 3-DOF formation. As illustrated in Figure 3, a_1, a_2 and a_3 are corresponds to the length of Link 1, Link 2 and Link 3. As expressed in (1) and (2), by using Denavit-Hartenberg conversion are used to convert from Cartesian coordinates into leg's joints polar coordinates

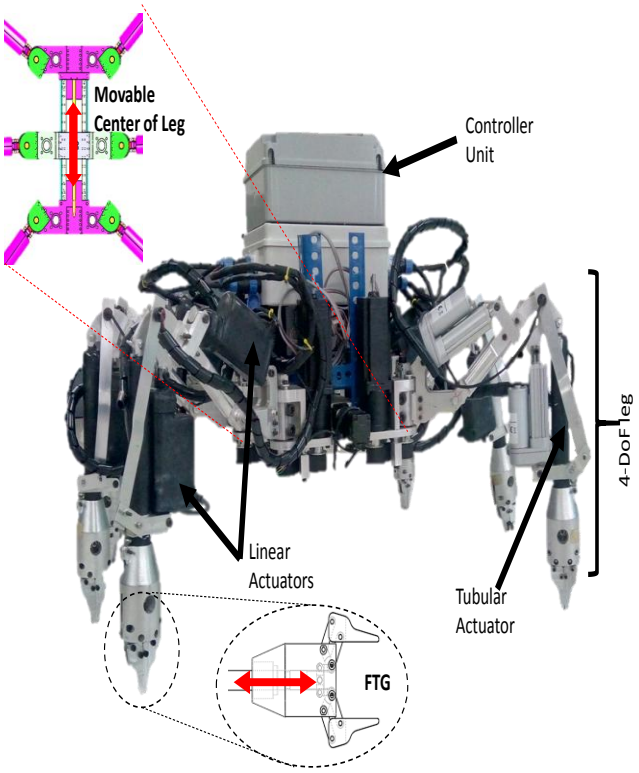

Fig. 2: Hexaquad robot [16]

Table 1: Actuator Specification Configured for Hexaquad Robot

Item	Value	Remarks
Linear actuator Load [N], Voltage Input [V] Current [Amp]	200, 12, 2	12 Unit
Tubular actuator Load [N], Voltage Input [V] Current [Amp]	200,12, 2	6 Unit
Bipolar Stepper, Torque [N/m], Voltage Input [V] Current [Amp]	54, 4.5, 3	6 Unit
Bipolar Stepper Motor (Body) Torque [N/m], Voltage Input [V] Current [Amp]	7.2, 24, 3	1 Unit

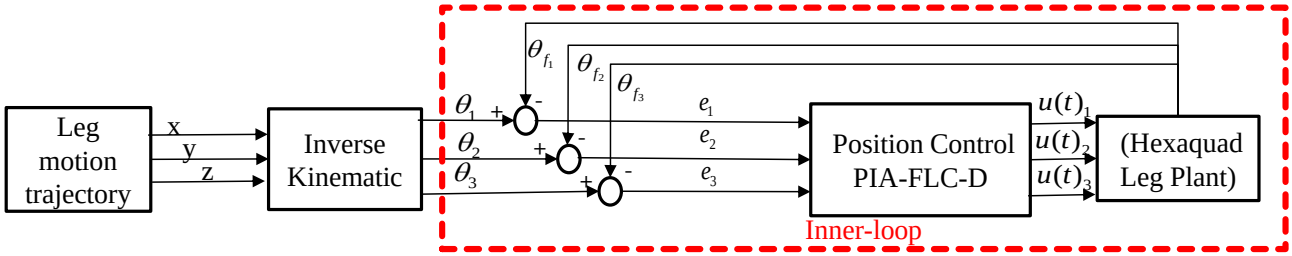

Fig. 4: Hexaquad's leg inner-loop control

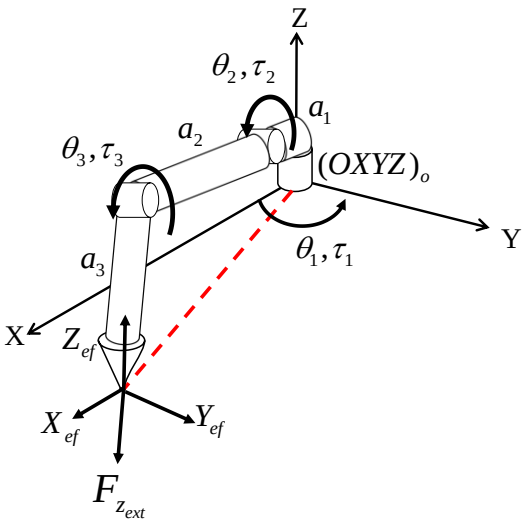

Fig. 3: Hexaquad's leg link orientation

$$\begin{pmatrix} x_e \\ y_e \\ z_e \end{pmatrix} = \begin{pmatrix} a_1\cos(\theta_1) + a_2\cos(\theta_1)\cos(\theta_2) + a_3\cos(\theta_1)\cos(\theta_{23}) \\ a_1\sin(\theta_1) + a_2\sin(\theta_1)\cos(\theta_2) + a_3\sin(\theta_1)\cos(\theta_{23}) \\ a_2\sin(\theta_2) + a_3\sin(\theta_{23}) \end{pmatrix} \quad (1)$$

$$\theta_3 = \cos^{-1}\frac{\left(\frac{x_e}{\cos(\theta_1)} - a_1\right)^2 + z_e^2 - a_2{}^2 - a_3{}^2}{2a_2a_3}$$

$$\theta_2 = \tan^{-1}\left(\frac{a_3\sin(\theta_3)}{a_2 + a_3\cos(\theta_3)}\right) + \sin^{-1}\left(\frac{z_e^2}{\sqrt{a_2 + a_3\cos(\theta_3)^2 + a_3\sin(\theta_3)^2}}\right) \quad (2)$$

$$\theta_1 = \tan^{-1}\left(\frac{x_e}{y_e}\right)$$

3. The Control Scheme for Hexaquad's Leg

3.1. Inner-Loop System of Hexaquad's Leg

Each Hexaquad's leg was designed with the same inner-loop architecture but with different parameters values as shown in Figure 4. The leg *i*th-joint position control were initially designed with Proportional Integral Antiwindup with Fuzzy Logic Control (PIA-FLC) [17], but later addition of derivative element is added to the controller to increase precision during walking motion trajectory tracking. For a successful walking, two primary sequences of walking were designed; lift to swing and drag. Concerning Figure 5, a walking motion with a semi-circle shaped was designed. The green arrow showed the direction of the tip of Hexaquad's leg movement and a dot indicates the starting point of walking motion for the Hexaquad's leg. During lift to swing sequence, T_{swing}, the robot required to lift up the leg and swinging toward the robot body whereas at dragging sequence, T_{drag}, the leg needs to imparting force to the environment so that robot can move to another location. The Cartesian coordinates of the designed motion were converted using (2) into leg's joint polar coordinates and feed to the inner-loop system. Note that, both sequences were designed to have similar motion speed.

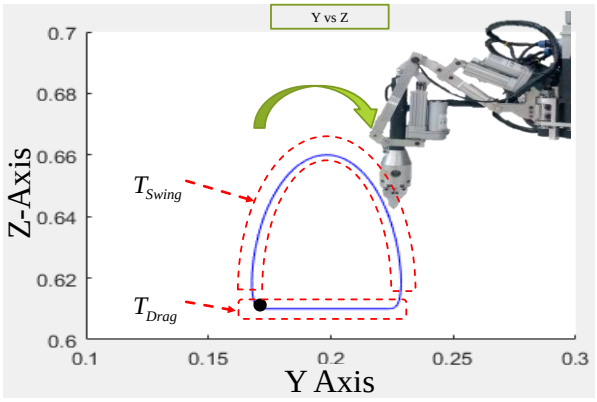

Fig. 5: Point of foot motion; two-dimensional semi-circle pattern

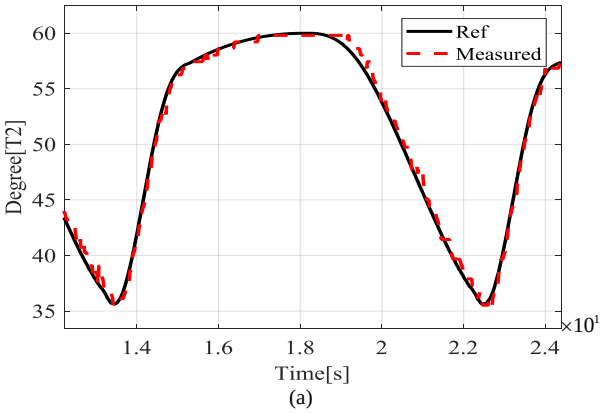

(a)

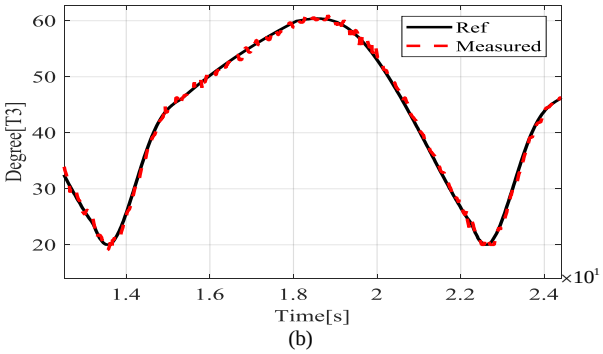

(b)

Fig. 6: Trajectory tracking (a) Joint 2 (b) Joint 3

As shown in Figure 5, the designed semi-circle pattern converted into joint's polar coordinates by inverse kinematics, only two from three joints of a Hexaquad's leg involved in translating the motion which is joint 2 and joint 3. As generated by inverse kinematics, the angular input for joint 1 is continuously zero since this joint significant affect x-axis of the leg whereas joint 2 and joint 3 simultaneously involved in y and z-axis respectively. Concerning the performance of inner-loop control during trajectory tracking as shown in Figure 6, the drag sequence is between 1.45 s to 1.9 s and between 1.9 s to 2.4 s is the swing sequence. As shown in Figure 6(a), at joint 2, a slight delay occurs at 1.9 s, but overall the modified PIA-FLC showed an excellent trajectory tracking for both joints.

3.2. Motion Speed Variation Control using Impedance Control Approach on Leg Dragging

Aforementioned, leg sank into the medium when it placed on soft terrain, e.g., mudflat. The leg will encounter difficulties in completing the motion especially during dragging sequence since it requires more energy to impart force to the muddy medium. Thus, the impedance control approach is designed for Hexaquad's leg to control the energy exchange of the leg with a speed variation of motion. The controller defined the relationship between force measured during foot placement and behavior of the leg end-effector $(xyz)_{ef}$ and its joints (θ_i), with $i = 1...3$. As shown in Figure 7, the input signal of impedance control is force error on the z-axis, e_f as in (3) which obtained by comparison between force sensor reading on the z-axis, F_{zf} and force reference, F_{zr} . Given that, $F_{zf} \geq F_{zr}$. In the 1980s, Hogan [18] introduced a system of second-order mass-damping-spring for impedance control that acts as a model reference as in (4),

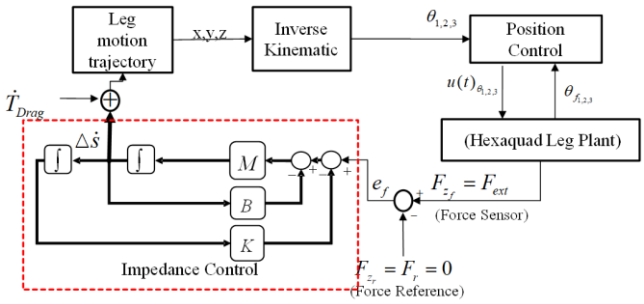

Fig. 7: Proposed impedance control for leg speed variation

$$e_f = F_{zf} - F_{zr} \tag{3}$$

$$|e_f| = M\Delta\ddot{a} + B\Delta\dot{s} + K\Delta s \tag{4}$$

where *M*, *B*, and *K* corresponds to parameters of mass, damping, and stiffness. As expressed in (4), $\Delta\ddot{a}$, $\Delta\dot{s}$ and Δs are representing an acceleration, velocity, and position output states respectively. Moreover, *M* is a total weight of the Hexaquad's leg, whereas *B* and *K* are unknown and tunable parameters. Hence, a damping ratio with a critically damped case ($\zeta = 1$) method is used to tune the parameters based on (5).

$$B = 2\sqrt{KM} \tag{5}$$

Since (5) expressed the mathematical relationship between three parameters, therefore, only *K* required being tuned to regulate the end-effector impedance behavior based on F_{zf} . Next, as shown in Figure 5, the resulting velocity state, $\Delta\dot{s}$ from impedance control is used to change leg motion speed, $\dot{T}_{drag}$ at dragging sequence only by changing the motion rate, ΔT_{drag}. Note that, $F_{zf} = F_{zr}$, the drag sequence motion rate, ΔT_{drag} is equal to the swing sequence motion rate, ΔT_{swing}.

4. Results and Discussions

4.1. Experimental Setup

The first leg of Hexaquad was selected as a platform to implement and experiment with the proposed motion speed controller. For safety precautions, an option to manipulate the F_{ext} by giving pressure directly to the first leg's force sensor using adjustable height chair as shown in Figure 8, was selected instead of applying the proposed controller to all Hexaquad's legs. Given that, $F_{zr} = 0$ and $F_{zf} = F_{ext}$. The position of the chair was fixed, and its surface is rotatable. Note that, the end effector of Hexaquad's leg (force sensor) will be touching the marked red area of the chair as shown in Figure 9. This setup is to allow the Hexaquad's leg to complete the drag phase by pushing the marked area while chair surface rotates in the direction shown by the red arrow in Figure 9. The sole objective of this experiment is to observe whether the leg link speed and energy increase as the force reading increases.

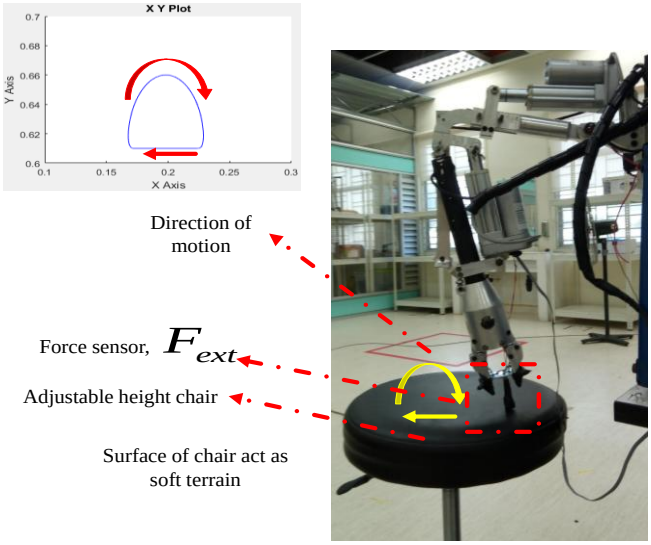

Fig. 8: Experiment setup

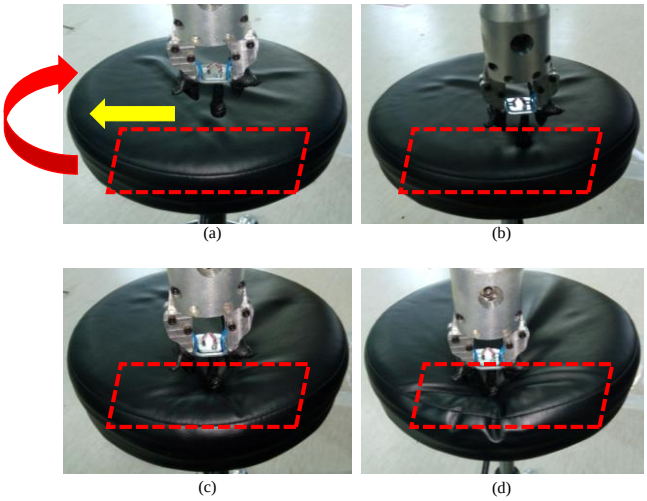

Fig. 9: Method obtaining force sensor reading; approximately (a) 0 N (b) 40 N (c) 80 N (d) 100 N

The chair's cushion act as the soft surface. The experiments parameters were set into two conditions; F_{ext} = 0 N and $F_{ext} \neq 0$ N where both conditions indicate force sensor does not contact with any surface and contacting with the surface respectively. For $F_{ext} \neq 0$ N, three set of experiments with different force reading were run to observe the behavior of the system, especially during drag sequence as shown in Figure 9. In each experiment, the leg movement is repeated for several cycles. On the other hand, in order to obtain the required external force reading, the height of the chair is increased during the experiment running until the approximate force reading achieved.

4.2. Experimental Results and Discussion

The performance of leg motion is evaluated by both its velocity and kinetic energy as shown in Figure 10. The black track indicates that F_{ext} = 0 N where it does not touch any surface, hence the velocity and kinetic value are similar to an initial set of the motion designed. However, as the height of the chair is increasing, it causing $F_{ext} \neq 0$ N due to sensor contacting the surface of the chair. Three selected reading to represent the effect of increasing force reading to the motion speed are at 40 N, 80 N and 100 N which were represented by tracks colored by red, green and blue respectively. Note that, in order to increase the velocity of the leg motion, the input trajectory requires to reduce the period of the sequence or increase the motion rate, ΔT. Thus, for all the experiments, ΔT_{swing} remain the same whereas ΔT_{drag} changes based on force reading. Concerning Figure 10(a), during drag sequence period as marked, the leg speed is increasing from 3.406 cm/s to 10.67 cm/s when external force increases from 0 to 100 N. On the other hand, the kinetic energy performances show also increasing when deeper foot to the ground whereby kinetic energy is increasing from 11.38 J to 146.9 J when force external increasing g from 0 N to 100 N respectively. The performance has validated the relationship between the velocity of the leg and its kinetic energy where the energy of the object increases as the moving object velocity increases.

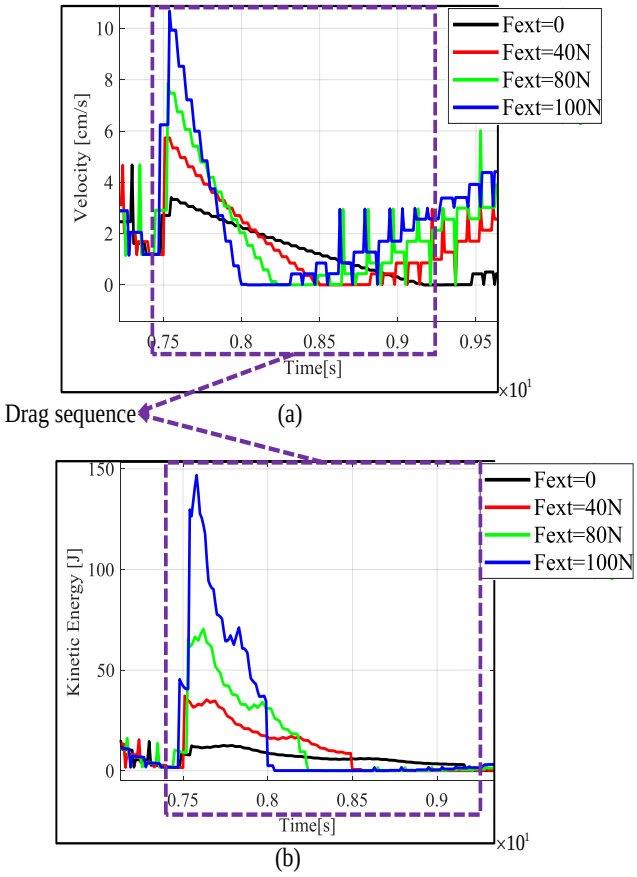

Fig. 10: Experimental results at drag sequence; (a) Velocity (b) Kinetic energy

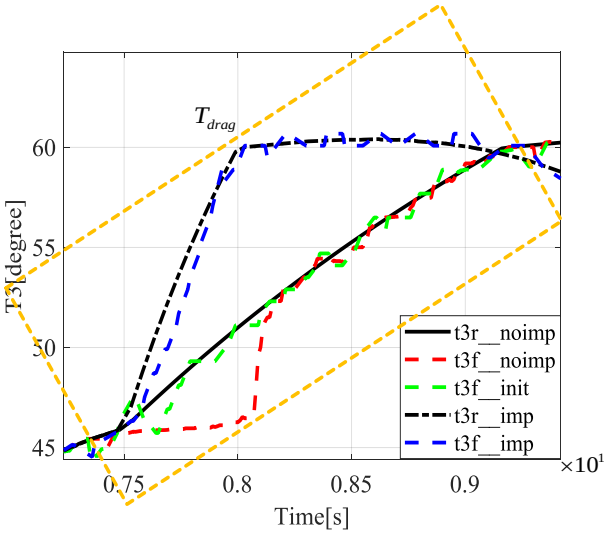

Fig. 11: Effect of velocity correction to the joint 3 of Hexaquad's leg

Further experimental has been done to indicate the velocity correction on the leg motion. As shown in Figure 11, the black track represents the initial motion track designed that capable of being followed by green track since F_{ext} = 0 N in which leg is hanging on air (no contact with the surface). However, when the leg was set touching the surface at approximately 100 N, joint 3 of Hexaquad's leg was unable to overcome the force acting on the leg causing the reading deviates from reference track. Thus the motion a bit disturbed as shown in Figure 11. This situation occurred due to the insufficient control input current generated by the position control. This unwanted scenario is not required for locomotion event. It is different when impedance control was deployed as shown in Figure 11 whereby the new velocity state from impedance control able to increase the motion rate, that resulting time reduction the in drag sequence. The dashed black track showed in Figure 11 indicates the new track to motion as the dragging period decreases. Also, the blue track showed that the leg capable of following the motion designed during trajectory tracking without changing the shape of the designed leg motion.

5. Conclusion

The performance of Hexaquad's leg with proposed speed variation control using a velocity-based impedance control on the soft surface is presented. With reference to the experimental results, the proposed control system is able to change the motion rate of designed motion instead of re-positioning the leg trajectory. This performance has increased the overall kinetic energy of the leg to impart more force to the environment, and this action had overcome the pressure acting on the leg. Moreover, the results showed that as the external force on foot increases, the velocity increases and corrected by impedance control in which $F_{ext} \neq 0$ N. The proposed control strategy is suitable to be deployed when the legged robot is carrying a different weight of payload during locomotion. For future work, this proposed method will be integrated with position correction so that it can adapt unstructured terrain with muddy type medium.

Acknowledgment

This research and development are supported by the Ministry Of Higher Education Malaysia under the Fundamental Research Grant Scheme(FRGS) (Grant No. FRGS/1/2016/TK04/UMP/02/9)

and Universiti Malaysia Pahang (UMP) Research Grant (RDU160147).

References

[1] Nonami K, Barai RK, Irawan A, & Daud MR (2014), *Hydraulically Actuated Hexapod Robots: Design, Implementation and Control*, Springer Netherlands.

[2] Kitano S, Hirose S, Horigome A, & Endo G (2016), "TITAN-XIII: sprawling-type quadruped robot with ability of fast and energy-efficient walking," *ROBOMECH Journal*, vol. 3, p. 8.

[3] Park JY, Shim H, Jun BH, Lee PM, Yoo SY, & Baek H (2017), "Measurement of hydrodynamic forces and moment acting on Crabster, CR200 using model tests," *2017 IEEE Underwater Technology (UT)*, pp. 1-5.

[4] Boaventura T, Buchli J, Semini C, & Caldwell DG (2015), "Model-Based Hydraulic Impedance Control for Dynamic Robots," *IEEE Transactions on Robotics*, vol. 31, pp. 1324-1336.

[5] Komati B, Pac MR, Ranatunga I, Clévy C, Popa DO, & Lutz P (2013), "Explicit force control vs impedance control for micromanipulation," *ASME 2013 International Design Engineering Technical Conferences and Computers and Information in Engineering Conference*, pp. V001T09A018-V001T09A018.

[6] Qin M, Xiao N, Guo S, Guo P, & Wang Y (2015), "A proximal push force-based force feedback algorithm for robot-assisted vascular intervention surgery," *Mechatronics and Automation (ICMA), 2015 IEEE International Conference*, pp. 738-742.

[7] Guo S, Wang P, Guo J, Wei W, Ji Y, & Wang Y (2013), "A novel master-slave robotic catheter system for Vascular Interventional Surgery," *Mechatronics and Automation (ICMA), 2013 IEEE International Conference*, pp. 951-956.

[8] Vukobratovic M (2009), *Dynamics and robust control of robot-environment interaction* vol. 2: World Scientific.

[9] Zhu YG (2014), "Research on leg compliance of multilegged walking robot based on impedance control," PhD, Zhejiang University.

[10] Ke X (2017), *Active/Passive Compliance Control for a Hydraulic Quadruped Robot Based on Force Feedback* vol. 53.

[11] Buchli J, Kalakrishnan M, Mistry M, Pastor P, & Schaal S (2009), "Compliant quadruped locomotion over rough terrain," *Intelligent Robots and Systems, 2009. IROS 2009. IEEE/RSJ International Conference*, pp. 814-820.

[12] Focchi M, Medrano-Cerda GA, Boaventura T, Frigerio M, Semini C, Buchli J, *et al.* (2016), "Robot impedance control and passivity analysis with inner torque and velocity feedback loops," *Control Theory and Technology*, vol. 14, pp. 97-112.

[13] Hyun DJ, Seok S, Lee J, & Kim S (2014), "High speed trot-running: Implementation of a hierarchical controller using proprioceptive impedance control on the MIT Cheetah," *The International Journal of Robotics Research*, vol. 33, pp. 1417-1445.

[14] Irawan A, Nonami K, & Daud MR (2013), "Optimal Impedance Control with TSK-Type FLC for Hard Shaking Reduction on Hydraulically Driven Hexapod Robot," *Autonomous Control Systems and Vehicles: Intelligent Unmanned Systems*, Eds., ed Tokyo: Springer Japan, pp. 223-236.

[15] Bjelonic M, Kottege N, & Beckerle P (2016), "Proprioceptive control of an over-actuated hexapod robot in unstructured terrain," *2016 IEEE/RSJ International Conference on Intelligent Robots and Systems (IROS)*, pp. 2042-2049.

[16] Irawan A & Tumari MZ (2014), "Hexa-Quad Robot with Prismatic Body Configuration and Leg-to-Arm Transformation," Malaysia Patent.

[17] Lezaini W, Irawan A, Razali A, & Adom A (2017), "Hybrid antiwindup-fuzzy logic control for an underactuated robot leg precision motion," *Robotics and Manufacturing Automation (ROMA), 2017 IEEE 3rd International Symposium*, pp. 1-6.

[18] Hogan N (1984), "Impedance control: An approach to manipulation," *American Control Conference*, pp. 304-313.